

SETTLEMENTS IN FINE-GRAINED SOILS UNDER CYCLIC LOADING

KAZUYA YASUHARA,ⁱ⁾ SATOSHI MURAKAMIⁱⁱ⁾, NORITAKA TOYOTAⁱⁱⁱ⁾ and ADRIAN F. L. HYDE^{iv)}

ABSTRACT

Based on the methods previously presented by the authors (Yasuhara et al., 1992, 1994, 1996) for predicting the degradation in strength and stiffness of soft clays in the course of cyclic loading, a methodology has been developed to estimate the cyclic loading-induced settlements. The method also includes not only immediate settlements but also post-cyclic long-term settlements due to dissipation of cyclically induced excess pore pressures in soft soils. The simplified formulae included in the proposed methodology are given as functions of the amplitude of cyclic-induced excess pore pressure normalized by the confining pressure, u/p'_c , plasticity index I_p and factor of safety against bearing capacity failure, F_s . The calculations of cyclic-induced settlements were conducted for soft soil deposits with different index and geotechnical properties. The results calculated using the proposed methodology are presented in the form of a design chart to give the settlement versus normalized excess pore pressure ratio relations including the effects of the plasticity index and safety factor for bearing capacity. An example of the calculated results using the proposed procedure for the earthquake-induced settlements of embankments founded on soft clay, is presented to demonstrate the practicality of the method for design at fields.

Key words: cyclic loading, excess pore pressure, fine grained soil, plasticity index, safety factor, settlement (IGC: D7/E8)

INTRODUCTION

In comparison with the cyclic behaviour of loose sand, soft cohesive soils are believed to be relatively stable, except for some previous case histories, because no liquefaction takes place in them even under strong motion from earthquakes. Instead, instantaneous settlements may occur, possibly leading to instability and inducing differential settlement of structures. Extreme cases were experienced in the 1957 and 1985 earthquakes in Mexico and the 1964 earthquake in Alaska. In addition to these cases, it has been reported that slopes of sensitive clay in Canada were damaged during the Sagueney earthquake in 1988 (Lefebvre et al., 1991), and lateral deformations occurred during the Loma Prieta earthquake in 1987 (Boulangier et al., 1998) due to cyclic softening of silt with a low plasticity index. From previous works the authors have noted that the damage in fine-grained soils is triggered not only by a reduction in strength but also by a degradation in stiffness (Yasuhara et al., 1994; Yasuhara and Hyde, 1997; Yasuhara et al., 1997; Yasuhara, 1999). As a consequence a methodology has been presented for constructing a design chart to evaluate earthquake-induced settlements of fine-grained soils. Reduction in strength and stiffness of fine-grained soils after undrained cyclic loading included in the method was

formulated from the results of cyclic triaxial tests and cyclic direct-simple shear (DSS) tests, and then this was taken into consideration in the methodology. The proposed procedure is practical in that it is given in terms of the factor of safety for bearing capacity, plasticity index and earthquake-induced excess pore pressures normalized by the confining pressure. The former two items are easily determined. On the other hand, the last item should be determined using dynamic analysis incorporated by a reliable and realistic constitutive relation. However, it should be noted that this aspect is not described in detail in the present paper. In order to estimate precisely, the distribution of u/p'_c which might occur during the actual earthquake should be determined using a reliable two- or three-dimensional dynamic numerical analysis.

EARTHQUAKE-INDUCED SETTLEMENTS IN SOFT GROUND

Earthquake-induced settlements should be considered separately for the two cases, the one with structures and the other without structures on the surface of the ground, as shown in Fig. 1. When we consider the former case as shown in Fig. 1, the settlements consist of both the immediate settlement, $\Delta S_{i,cy}$, which is observed just

ⁱ⁾ Professor, Department of Urban and Civil Engineering, Ibaraki University, 4-12-1 Nakanarusawa, Hitachi 316-8511, Japan.

ⁱⁱ⁾ Research Assistant, ditto.

ⁱⁱⁱ⁾ Civil Engineer, Tokyo Electrical Power Co., Ltd., Tokyo, Japan.

^{iv)} Senior Lecturer, University of Sheffield, Sir Frederick Mappin Building, Mappin Street Sheffield S1 3JD, UK.

Manuscript was received for review on April 3, 2000.

Written discussions on this paper should be submitted before July 1, 2002 to the Japanese Geotechnical Society, Sugayama Bldg. 4F, Kanda Awaji-cho 2-23, Chiyoda-ku, Tokyo 101-0063, Japan. Upon request the closing date may be extended one month.

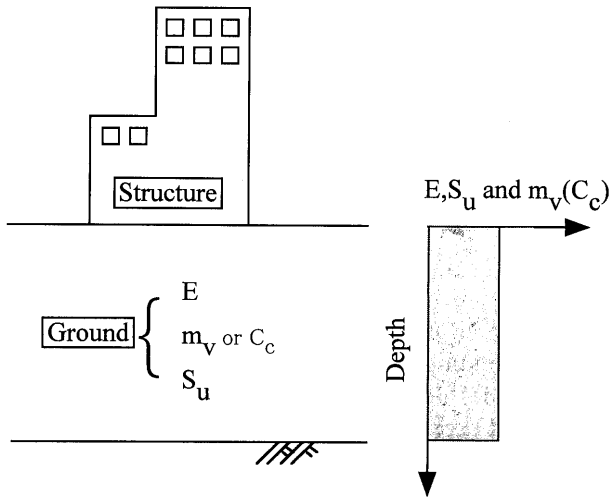


Fig. 1. Sketch of ground with building structure

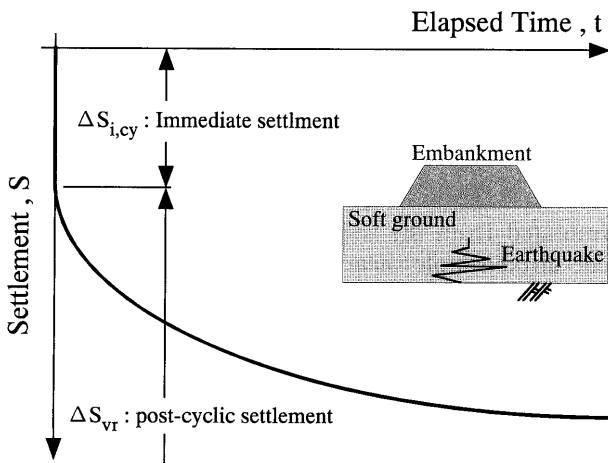


Fig. 2. Sketch of earthquake-induced settlement of embankment on soft ground

after an earthquake, and the post-earthquake recompression settlement, ΔS_{vr} , due to dissipation of cyclic-induced excess pore pressures. Thus, as shown in Fig. 2 the total incremental settlement, ΔS_{cy} , of ground with structures under earthquakes is generally given by:

$$\Delta S_{cy} = \Delta S_{i,cy} + \Delta S_{vr} \quad (1)$$

It is indicated from the previous studies (Hyodo et al., 1994; Yasuhara et al., 1997) that excess pore pressure generation in soft ground with structures during earthquakes decreases with increasing initial shear stress (ISS) induced by structures. This can be understood in Fig. 3 which schematically illustrates the effective stress paths and the void ratio versus mean effective principal stress relations in a soil element with and without initial shear stress, during earthquakes. However, residual settlements increase due to the initial shear stress which makes the cyclic strength of clays decrease (Hyodo et al., 1994, 1998) as well as inducing the large inertial forces triggered by the motions of the structure under earthquake

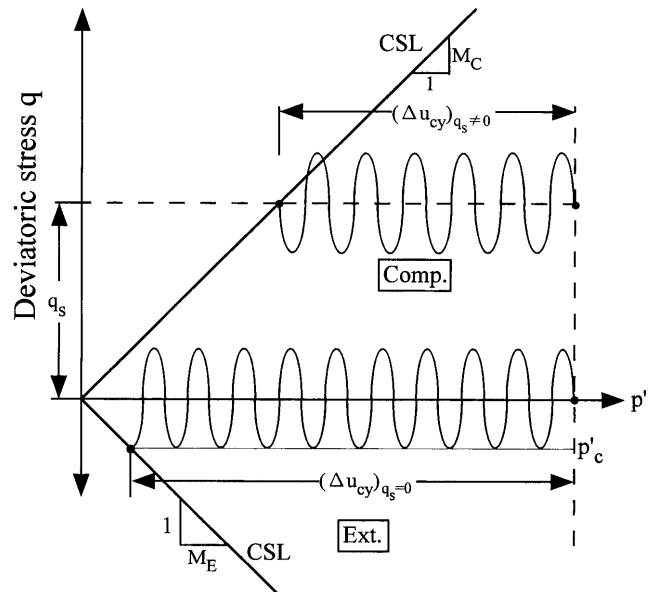
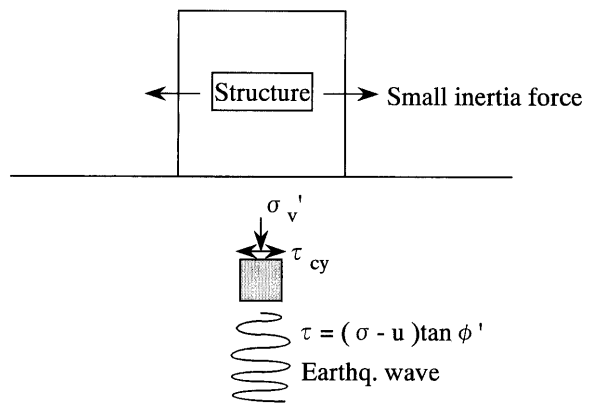
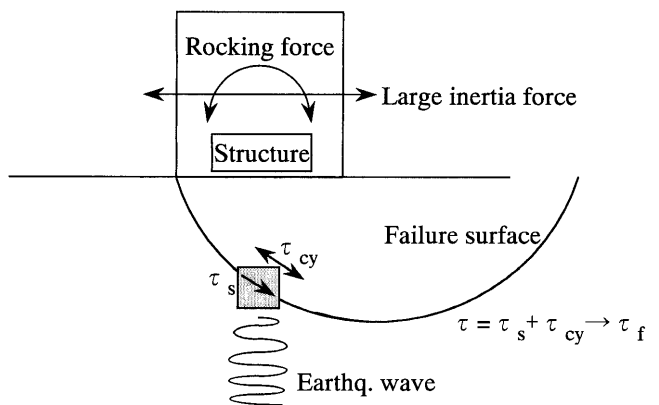


Fig. 3. Excess pore pressures generated during undrained cyclic loading with and without initial static shear stress



(a) Liquefaction of sand



(b) Cyclic failure of clay

Fig. 4. Comparison between liquefaction of sand and cyclic failure of clay (after Hyodo et al., 1994)

conditions. This may produce large shear stresses and deformation leading to failure (see Fig. 4). It is reported that settlements and deformation in level soft clay grounds, and displacements in sensitive clay slopes have been observed during earthquakes such as the 1964 Alaska, 1985 Michiocan, and 1987 Loma Prieta.

Although in the case without a structure on the ground surface, instantaneous settlements would not normally be observed, post-earthquake recompression settlements might sometimes be significant because larger excess pore pressures are generated than in the case with a structure on the ground. Post-liquefaction recompression settlements in sands occur very rapidly due to the immediate dissipation of cyclically induced pore pressures, equal to the vertical overburden stress after liquefaction. In the case of fine-grained soils, on the other hand, it sometimes takes a long time for earthquake-induced excess pore pressures to dissipate even if lower excess pore pressures may have been generated during earthquakes (Zeevaert, 1987; Matsuda, 1998). Case histories pertaining to settlements of this kind have been recorded after some previous earthquakes and methods for predicting them have also been proposed (Ohara and Matsuda, 1989; Yasuhara, 1995; Pradhan et al., 1997).

A METHOD FOR EVALUATING EARTHQUAKE-INDUCED RESIDUAL SETTLEMENTS IN SOFT GROUND

Immediate Settlement

Figure 5 is a key figure for the interpretation of the effect of cyclic loading on load intensity versus settlement curves observed in level soft ground. Curve I is for static loading with no cyclic loading and Curve II corresponds to a case with earthquake loading. If this soft ground con-

sisted of loose saturated sand, the bearing capacity would decrease immediately and large displacements might occur due to large earthquakes. We would then have Curve III since, in comparison with fine-grained soils, loose saturated sands are very sensitive to cyclic loading. However, even if the soft ground consists of a fine-grained soil, the effective stress decreases due to excess pore pressure generation and this induces some instability depending upon the severity of cyclic loads and initial shear stresses.

Let us, now, assume we have a structure with $q(=q_{f,NC}/F_s)$ as an average load intensity on the soft ground in which the load versus settlement relation follows Curve I before and Curve II after an earthquake, respectively, as shown in Fig. 5. Since both the strength and stiffness of the ground degrade, additional settlement, $\Delta S_{i,cy}$, takes place due to an earthquake-induced decrease of effective stress corresponding to a shift from A to B in Fig. 5. It is assumed that the load versus settlement Curves I and II before and after earthquakes are formulated in terms of the hyperbolic function respectively given by (Yamaguchi, 1977; Kusakabe and Kawai, 1989):

$$S_{i,NC} = \frac{q_{f,NC}q}{K_{i,NC}(q_{f,NC} - q)} \quad (2a)$$

$$S_{i,cy} = \frac{q_{f,cy}q}{K_{i,cy}(q_{f,cy} - q)} \quad (2b)$$

where $K_{i,NC}$ and $K_{i,cy}$ are ground reaction coefficient before and after cyclic loading, respectively. Combination of Eq. (2a) with Eq. (2b) leads to:

$$\frac{\Delta S_{i,cy}}{S_{i,NC}} = \frac{R_q}{R_K} \left(\frac{1 - \frac{1}{F_s}}{R_q - \frac{1}{F_s}} \right) - 1 \quad (3)$$

where $\Delta S_{i,cy}$ is equal to $(S_{i,cy} - S_{i,NC})$, $R_q = q_{f,cy}/q_{f,NC}$, $R_K = K_{i,cy}/K_{i,NC}$ and F_s is the safety factor for bearing capacity. By postulating that R_q and R_K are equal to the undrained strength ratio, $s_{u,cy}/s_{u,NC}$ and initial secant stiffness ratio, $E_{s,cy}/E_{s,NC}$, respectively, we can adopt the following relations previously proposed by the just author (1994a, 1994b) and authors (1997):

$$R_q = \frac{s_{u,cy}}{s_{u,NC}} = n_q^{A_0/(1-C_s/C_c)} - 1 \quad (4a)$$

$$R_K = \frac{K_{i,cy}}{K_{i,NC}} = \frac{E_{s,cy}}{E_{s,NC}} = \frac{1 - \frac{C}{A} \ln n_q}{n_q} \quad (4b)$$

where A is $1 - C_s/C_c$ (C_s and C_c are the swelling and compression indices respectively), and A_0 is the strength ratio parameter, given as (Mitachi and Kitago, 1976):

$$A_0 = \frac{\log \left[\frac{(s_u/p')_{OC}}{(s_u/p')_{NC}} \right]}{\log(OCR)} \quad (5)$$

C is also experimental constant, and is defined as (Wroth

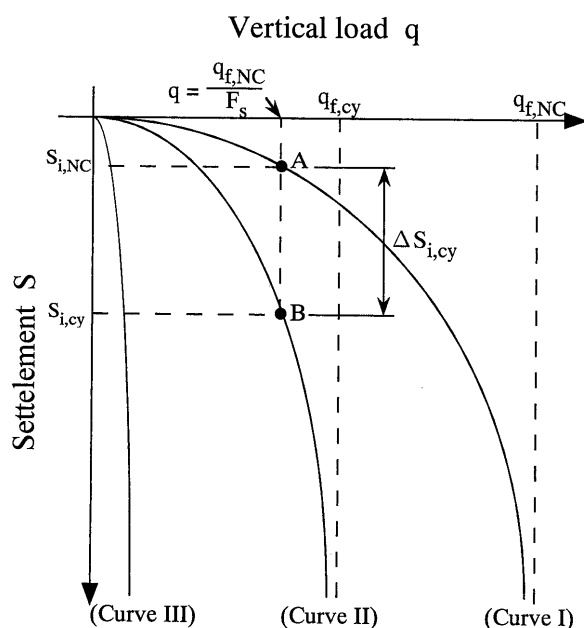


Fig. 5. Instantaneous settlement of structures on soft ground due to undrained cyclic loading

and Houlsby, 1985):

$$C = \frac{\left[\frac{(E/p')_{OC}}{(E/p')_{NC}} \right] - 1}{\ln OCR} \quad (6)$$

while n_q is defined as:

$$n_q = \frac{1}{1 - \frac{u}{p'_c}} \quad (7)$$

Finally $s_{u,NC}$, $s_{u,cy}$ are the undrained strengths before and after cyclic loading respectively, and $E_{i,NC}$, $E_{i,cy}$ are the undrained secant moduli before and after cyclic loading. Both Eqs. (4a) and 4(b) were derived from:

$$K = \frac{E}{(1 - \nu^2)BI_p} \quad (8a)$$

$$q_f = (2 + \pi)s_u \quad (8b)$$

The detailed derivations for Eq. (4a) and Eq. (4b) from the above two relations (8a) and (8b) have already been described in previous papers (Yasuhara et al., 1992, 1994, 1997). The applicability of both Eqs. (4a) and (4b) has been verified. The results will be presented later. When we combine Eqs. (4a) and (4b) with Eq. (3), Eq. (3) can be a simple function of u/p'_c and F_s .

Post-Earthquake Long-Term Settlement

When earthquake loading is terminated, excess pore pressure generated during undrained cyclic loading tends to dissipate, and then recompression takes place due to dissipation. Following Fig. 6, the void ratio decrement, Δe_{vr} , due to the effective stress recovering from p' (or σ'_{vc}) to p'_c (or σ'_v), followed by the dissipation of cyclic-induced excess pore pressures is given by:

$$\Delta e_{vr} = C_{r,cy} \log(p'_c/p'): \text{ for cyclic triaxial tests} \quad (9a)$$

$$\Delta e_{vr} = C_{r,cy} \log(\sigma'_{vc}/\sigma'_v): \text{ for cyclic DSS tests} \quad (9b)$$

where $C_{r,cy}$ is the recompression index for the state path from B to C in Fig. 6 during the dissipation of cyclic-induced excess pore pressures, and p'_c or σ'_{vc} and p' or σ'_v are effective vertical stress before and after cyclic loading, respectively. According to a previous investigation using cyclic DSS tests on Drammen clay (Yasuhara and Andersen, 1991), recompression index $C_{r,cy}$ is approximately related to the ordinary recompression index, C_r as:

$$C_{r,cy} = 1.5C_r \quad (10)$$

Also, when we assume $C_r = 0.15 \cdot C_c$ from the data collected by NGI (1991), and by Yasuhara and Andersen (1991), Eq. (10) becomes:

$$C_{r,cy} = 0.225 \cdot C_c \quad (11)$$

Thus, if we have a soft clay layer with height H , post-cyclic recompression settlement ΔS_{vr} is reduced to:

$$\Delta S_{vr} = 0.225H \frac{C_c}{1 + e_0} \log n_q \quad (12)$$

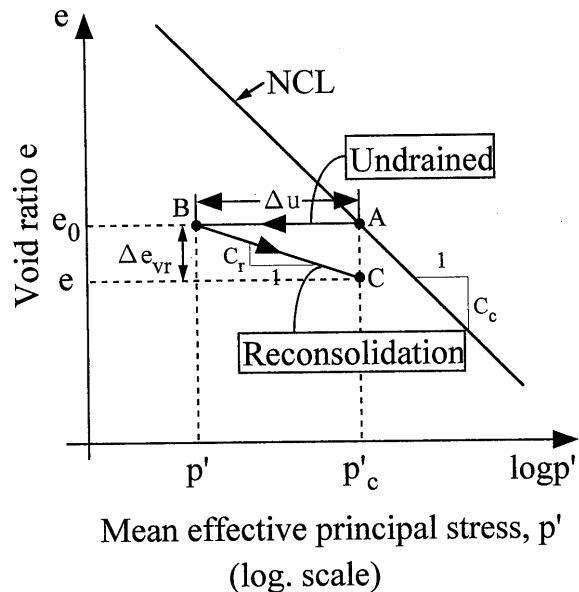


Fig. 6. Recompression settlement due to dissipation of cyclic-induced excess pore pressures

where C_c can be related to I_p :

$$C_c = 0.0348 + 0.0162 \cdot I_p \quad (13)$$

as proposed by Iizuka and Ohta (1986).

DESIGN CHART

Formulation for Total Settlement

By substituting Eq. (3) and Eq. (12) into Eq. (1), earthquake-induced settlements, ΔS_{cy} are given by:

$$\Delta S_{cy} = \Delta S_{i,cy} + \Delta S_{vr} = f_1 S_{i,NC} + f_2 \{ H / (1 + e_0) \} \quad (14)$$

where

$$f_1(u/p') = \frac{R_q}{R_k} \left[\frac{1 - 1/F_s}{R_q - 1/F_s} \right] - 1 \quad (15a)$$

$$f_2(u/p') = 0.225 C_c \log n_q \quad (15b)$$

The earthquake-induced settlements of structures founded on fine-grained soils as was previously shown in Fig. 1 and the inset in Fig. 2 can be calculated using Eq. (14) through Eqs. (15a) and (15b) when the following information is known:

- i) load intensity q , and the average width of the structure, B
- ii) plasticity index I_p , initial water content w_i (or initial void ratio, e_0) and depth of layers of the soil
- iii) soil strength, s_u , stiffness, E , and compressibility, C_c , and their variation with depth
- iv) magnitude and distribution of earthquake-induced excess pore pressures.

Among the above, earthquake-induced excess pore pressures should be determined using a dynamic response analysis with the non-linear stress-strain relation taken into consideration.

For simplicity, it is postulated in the present calcula-

tion that compression index, C_c , undrained strength, s_u , and Young's modulus, E , included in the procedure are constant with depth as shown in Fig. 1. The parameters included in Eq. (4a) and Eq. (4b) can be determined in terms of the plasticity as:

$$A_0 = 0.757 - 3.49 \times 10^{-3} I_p + 4.0 \times 10^{-6} I_p^2 \quad (16a)$$

$$A = 1 - C_s / C_c = 0.815 - 0.002 I_p \quad (16b)$$

These are obtained by combining the following empirical relations proposed by Ue et al. (1991)

$$\frac{A_0}{(1 - C_s / C_c)} = 0.939 - 0.002 I_p \quad (17a)$$

$$C_s / C_c = \lambda = 0.185 + 0.002 I_p \quad (17b)$$

These were based on the results in Figs. 7(a) and 7(b) which were obtained from previous studies including those parameters. In addition, Eq. (12) can be used for determination of compression index, C_c .

Construction of Design Chart

In order to construct a design chart for use by field engineers, calculations using the above-stated procedure were conducted by assuming values of F_s and I_p given as:

- i) $F_s = 1.25, 1.5, 2.0, 3.0$
- ii) $I_p = 0, 10, 20, 40, 60, 80, 100, 150, 200, 250, 300$

Figures 8(a) to 8(d) were then obtained as design charts in which two functions f_1 and f_2 are correlated to the normalized cyclic-induced excess pore pressure, u/p'_c . As a general trend, it can be seen from Fig. 8(a) through Fig. 8(d) that:

- 1) The immediate settlement ratio f_1 increases with increasing normalized cyclic-induced excess pore pressure, u/p'_c . In particular, the settlement ratio dramatically increases when u/p'_c reaches approximately 0.75, particularly when F_s is assumed to be large, such as equal to 3.0. This corresponds with the fact

that soft clays in undrained cyclic triaxial or constant volume DSS tests on normally-consolidated clay reach failure once the normalized excess pore pressure becomes 0.7 to 0.75 (Yasuhara et al., 1992; Hyodo et al., 1994).

- 2) The settlement ratio accelerates with increasing normalized excess pore pressure and decreasing safety factor. This tendency is eminent with increasing I_p .

In addition to the general design chart for practical use, the effects of safety factor on f_1 and f_2 versus u/p'_c relations were investigated using Eqs. (15a) and (15b) for reconstituted and undisturbed Ariake Clay, whose index properties are summarized in Table 1. Note that the index properties of the Ariake clays used are different since both specimens were sampled from different locations. The results calculated are presented in Figs. 9(a) and 9(b) for the cases of determining parameters both from triaxial tests and I_p using Eqs. (7a) and (7b). It is emphasized from Fig. 9(a) for reconstituted Ariake clay and Fig. 9(b) for undisturbed Ariake clay that:

- i) Both immediate and post-cyclic recompression settlements of fine-grained cohesive soils with high plasticity index increase with increasing plasticity index at the same magnitude of cyclic-induced excess pore pressure.
- ii) The overall agreement in f_1 versus u/p'_c relations is not observed between both cases of adopting parameters obtained from experiments directly and I_p indirectly. However, the f_1 versus u/p'_c curves for both cases become closer as the safety factor becomes larger.
- iii) On the other hand, f_2 versus u/p'_c relations are in good agreement with results from both cases using parameters from experiments and I_p .

By re-plotting the settlement ratio $\Delta S_{i,cy} / S_{i,NC}$ versus normalized pore pressure u/p'_c relations on a semi-logarithmic scale for Ariake clay as in the example shown in Fig. 10, it is possible to determine the inflection point

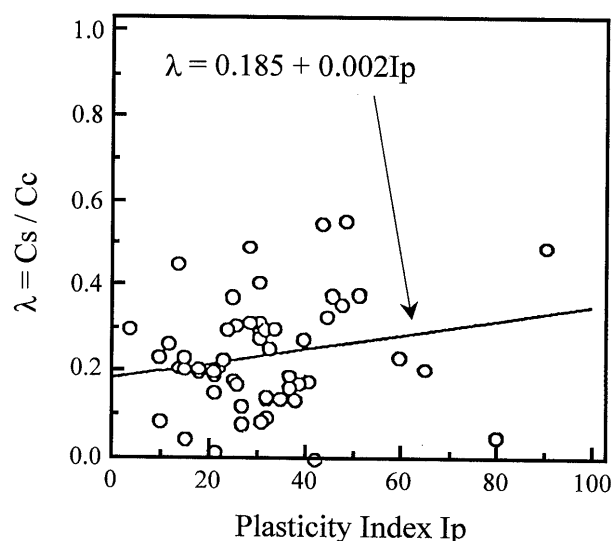
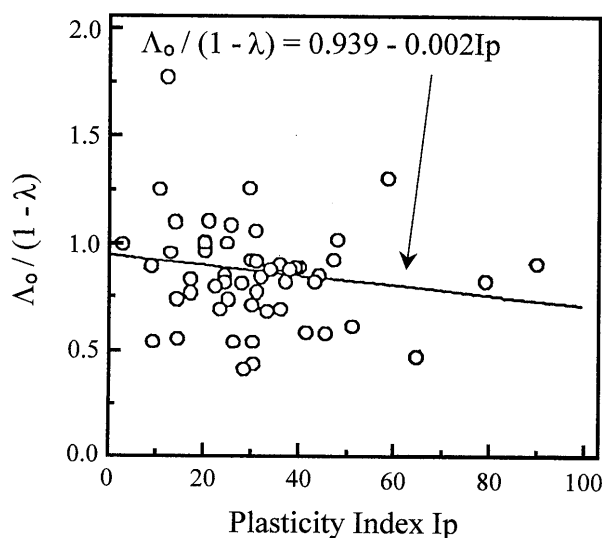


Fig. 7(a),(b). Two parameters $\Lambda_0 / (1 - \lambda)$ and $\lambda (= C_s / C_c)$ related to plasticity index

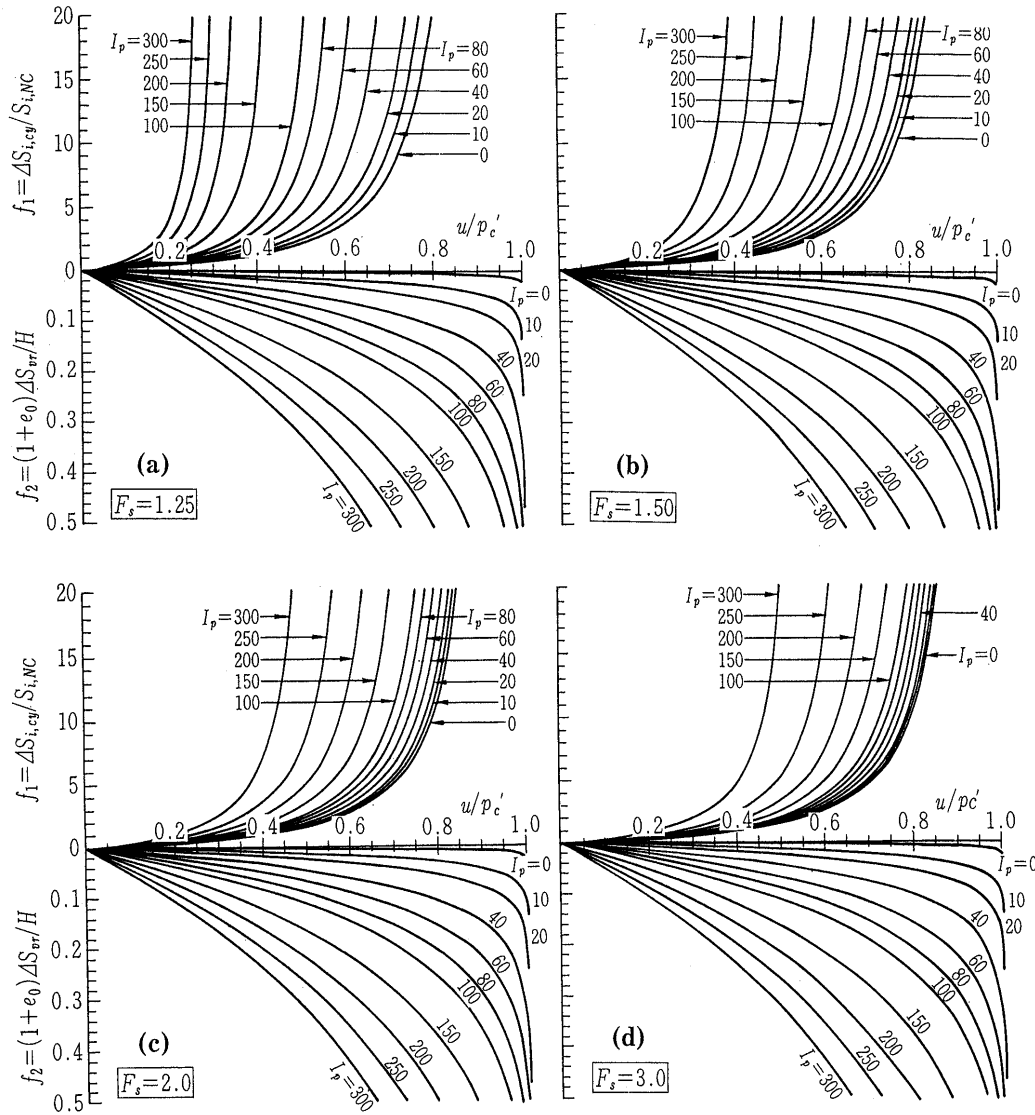


Fig. 8. Settlement ratio determined as functions of F_s and I_p plotted against normalized cyclic-induced excess pore pressure

Table 1. Parameters used for calculation

<Case I: Ariake clay (Reconstituted)>

	C_c	C_s	C_s/C_c	A_0	C
From experiment	0.845	0.158	0.187	0.767	0.26
From I_p ($I_p=58$)	0.974	—	0.301	0.568	0.26

<Case II: Ariake clay (Undisturbed)>

	C_c	C_s	C_s/C_c	A_0	C
From experiment	1.410	0.153	0.109	0.767	0.26
From I_p ($I_p=98$)	1.606	—	0.379	0.456	0.26

which corresponds to the critical value of normalized excess pore pressure, $(u/p'_c)_{CRT}$, where immediate settlements accelerate, as is schematically shown in Fig. 10. This critical value of excess pore pressures designated by $(u/p'_c)_{CRT}$ is plotted against plasticity index I_p for each

soil in Fig. 11 for different safety factors, F_s . The critical value $(u/p'_c)_{CRT}$ tends to decrease after the plasticity index I_p reaches 70 to 100. This tendency is more evident for the smaller values of safety factor.

An example of the influence of the earthquake-induced normalized excess pore pressures, u/p'_c , on the relation between settlement ratio, $\Delta S_{i,cy}/S_{i,NC}$, and the inverse value of F_s equal to the load intensity ratio (LIR), $q_{i,NC}/q$, is illustrated in Fig. 12 for Mexico City clay. It is indicated in Fig. 12 that the LIR corresponding to the point for the drastic increase in $\Delta S_{i,cy}/S_{i,NC}$ decreases with the increasing u/p'_c value produced during earthquakes.

Figure 13 shows the calculated variations of the settlement ratio with the load intensity induced by the self-weight of structures equal to the inverse value of safety factor ($1/F_s = q/q_{i,NC}$), for three specific values, 0.1, 0.3 and 0.5 of u/p'_c . From Fig. 13 it can be seen that:

- 1) Although the settlement ratio in soils with a low to medium plasticity index less than approximately 70 is almost constant, with values between 1.0 and 2.0,

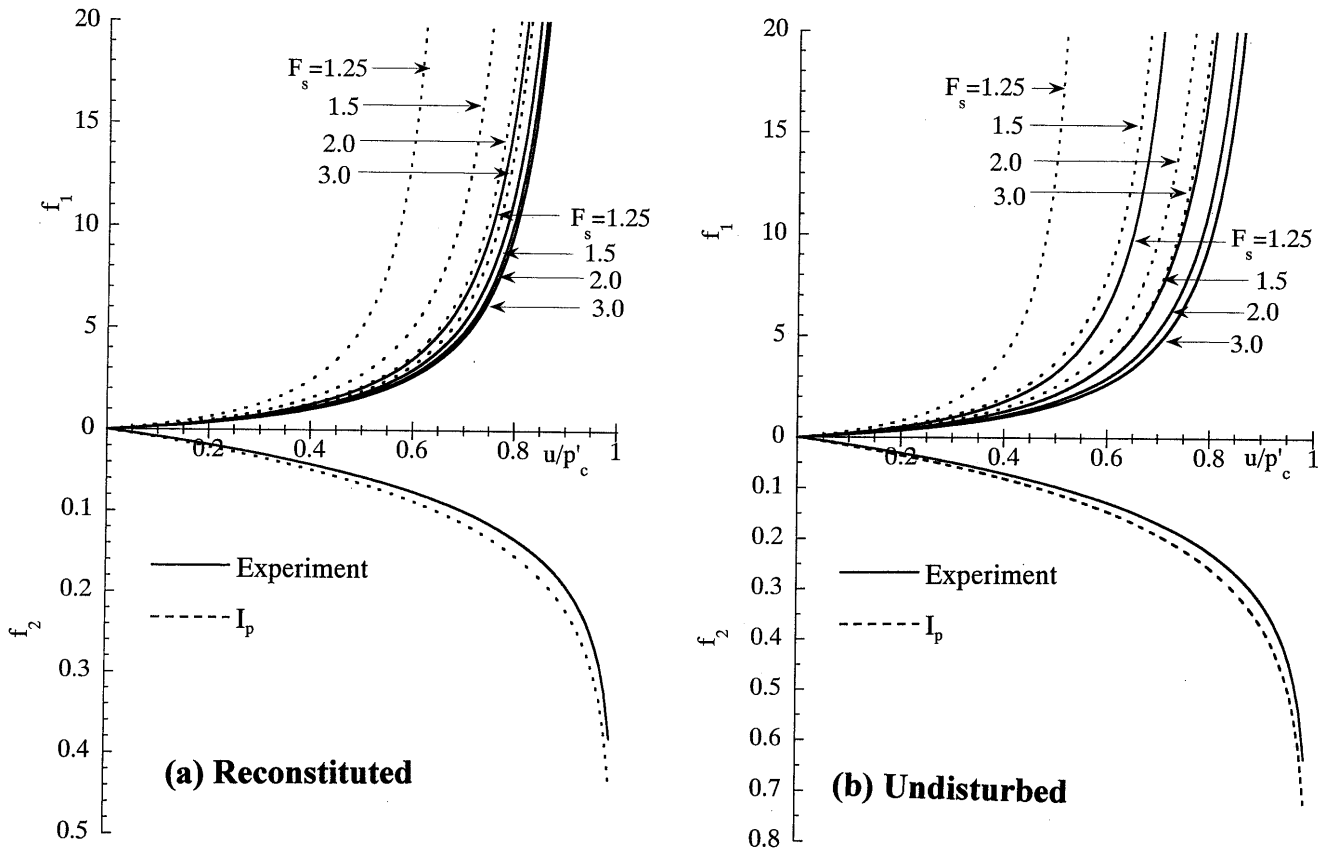


Fig. 9(a),(b). Effects of parameter determination on relation between settlement ratio and normalized excess pore pressure ratio for Ariake clay

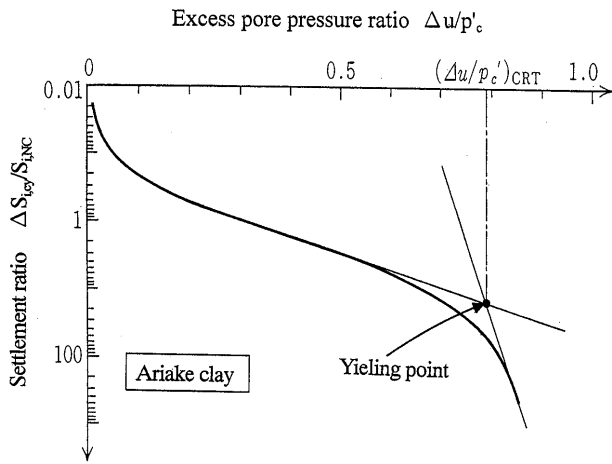


Fig. 10. Inflection point between settlement ratio and normalized excess pore pressure ratio

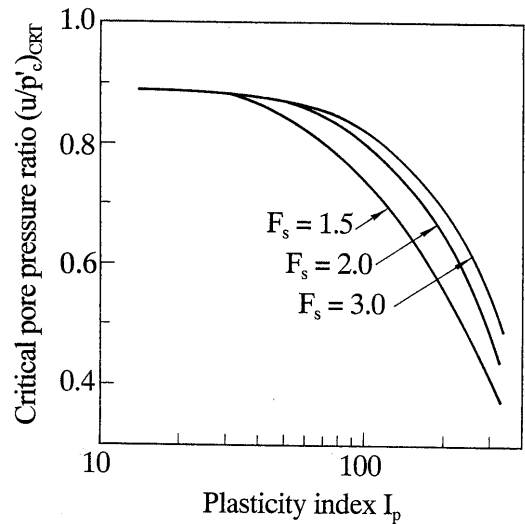


Fig. 11. Safety factor dependence on relation between critical value of normalized excess pore pressure and plasticity index

until the load intensity ratio ($LIR = 1/F_s$) becomes the critical value, i.e., 0.75, beyond this critical value it suddenly increases.

- 2) In other words, it is suggested that we had better use a value of safety factor larger than 1.33 to avoid large settlements due to strong earthquakes.

Also, the influence of plasticity index on the relation between $\Delta S_{i,cy}/S_{i,NC}$ and LIR is included in Fig. 13 for the specific value of u/p'_c generated during earthquakes. It is understood from Fig. 13:

- i) The value of LIR corresponding to the accelerated value of $\Delta S_{i,cy}/S_{i,NC}$ decreases with the increase of u/p'_c .
- ii) This tendency becomes eminent with an increasing plasticity index.

EXAMPLES OF APPLICATION

Ground Conditions for Calculation

To demonstrate the application of the proposed method, the profile of an embankment founded on soft ground is assumed to be as shown in Fig. 14. As is shown in Fig. 14, the ground at this site consists of a homogeneous plastic silt 30 m deep for which the representative index properties and mechanical parameters listed in Tables 1 and 2 are assumed to be constant throughout the underlying ground.

Cyclic and Post-Cyclic Properties of Arakawa Clay

The index properties of a fine-grained soil called Arakawa clay used to model the ground in dynamic centrifuge tests (Matsuo et al., 1997) are $\rho_s=2.67 \text{ Mg/m}^3$, $w_L=45.1\%$, $I_p=19.6$. Monotonic constant volume direct-simple shear (DSS) tests with a shear strain rate of 0.1%/min and stress-controlled cyclic DSS tests were conducted to obtain static and cyclic strength, and cyclic stiffness designated by Young's modulus. Post-cyclic monotonic tests were also carried out on specimens, which did not fail during undrained cyclic loading, to detect the changes in strength and stiffness after undrained

cyclic loading. Typical results from cyclic DSS tests followed by monotonic tests on normally-consolidated specimens of Arakawa silt are given in the form of $S_{u,cy}/S_{u,NC}$ and $G_{s,cy}/G_{s,NC}$ versus u/σ'_{vo} , respectively, and are shown in Fig. 15. It is to be noted that $G_{s,cy}/G_{s,NC}$ is used instead of $E_{s,cy}/E_{s,NC}$ in Fig. 15. The thick lines in Fig. 15 were obtained using Eq. (4a) and Eq. (4b), respectively. The parameters included in both equations are listed in Table 2 and Table 3.

Immediate Settlement due to Embankment

There have been several methods proposed for estimating immediate settlements due to self-weight of structures. Among them, a method proposed by Inada et al. (1977) was adopted for estimating the immediate or instantaneous settlement of foundations or structures on soft ground, as shown in Fig. 16. This is given as:

$$S_{i,NC} = \left(\frac{q}{E_i} \right) N_i \quad (17)$$

where q is the embankment load intensity, equal to $\gamma_i H_E$ (kN/m^2), E is the secant Young's modulus (kN/m^2) and N_i is the coefficient of immediate settlement. If the design chart by Inada et al. shown in Fig. 16 is used, we have $N_i=11.2 \text{ m}$ corresponding to $B/D=11/30=0.367$ from Fig. 16. The value of E_i/s_u was determined from the results of monotonic undrained triaxial tests (axial strain rate $\epsilon=0.1\%/min$) on reconstituted silty clay which was taken from the site. The results are shown in Fig. 17. The

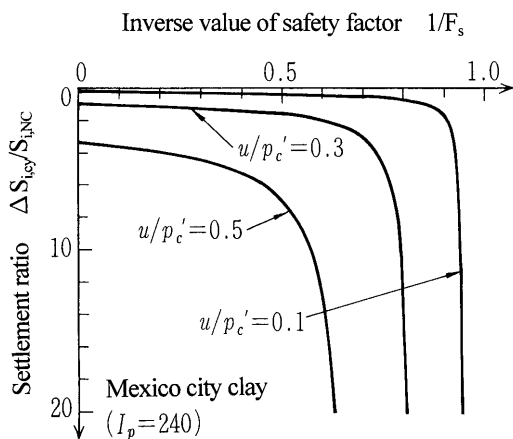


Fig. 12. Effect of normalized cyclic-induced excess pore pressure on relation between settlement ratio and $1/F_s$ for Mexico city clay

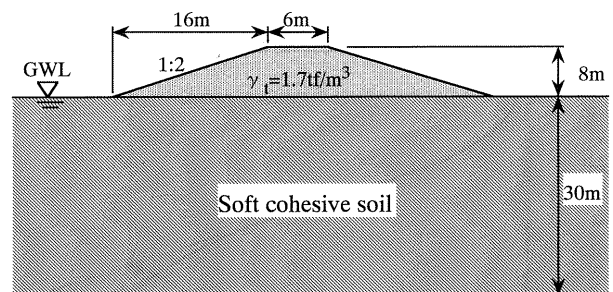


Fig. 14. Model for levee founded on soft ground used for calculation

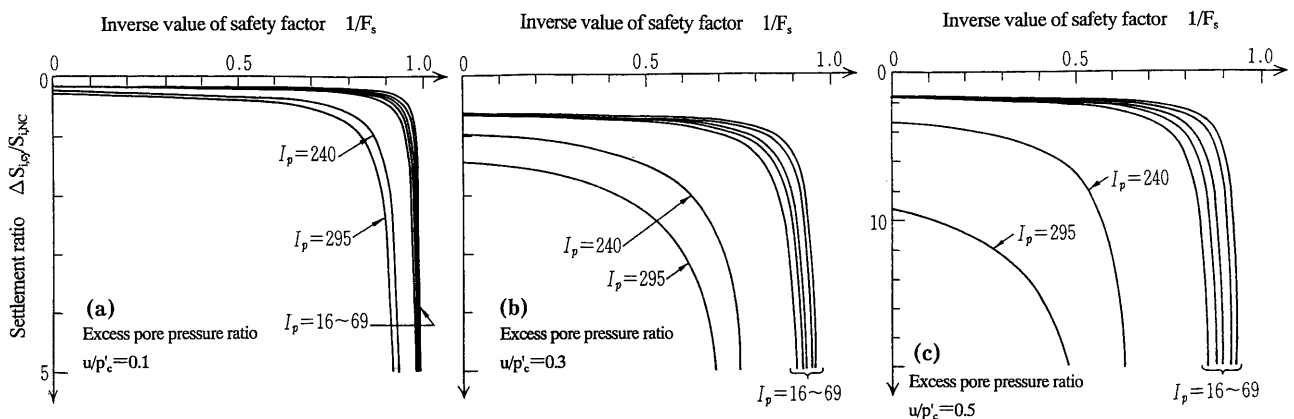


Fig. 13. Effects of cyclic-induced normalized excess pore pressure and plasticity index on relation between settlement ratio and $1/F_s$

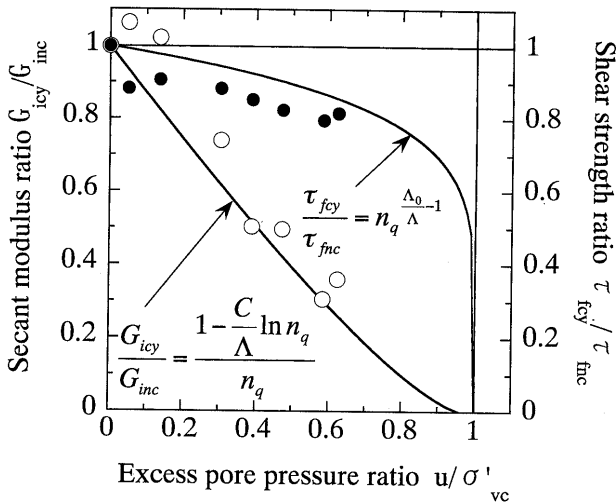


Fig. 15. Post-cyclic secant modulus ratio and undrained strength of silty clay obtained from post-cyclic DSS tests

Table 2. Scales of levee and ground

Height of levee H_E (m)	Gradient of slope	Width of top (m)	Representative width B (m)	Thickness of layer D (m)
8.0	1:2	6.0	11.0	30

Table 3. Index properties of levee and ground

Unit weight of levee γ_{tE} (tf/m ³)	Load intensity $\gamma_{tE} \times H_E$ (kPa)	Undrained strength s_u (kPa)	Stiffness index E_{50}/s_u
1.70	133.4	31.9	550

average undrained shear strength is assumed to be 31.9 kPa (half of the average unconfined undrained peak stress) which was obtained from a previous site investigation given in Fig. 18. Thus, the average secant Young's modulus of 17.6 MPa was determined. When we insert these values of q , E_{50} and N_i into Eq. (17), we obtain: $S_{i,NC} = 8.6$ cm.

Immediate Settlement due to Earthquakes

Since it was assumed in the present calculation that strength, deformation modulus and compressibility are kept constant against depth of the ground, bearing capacity, $q_{t,NC}$, was obtained as 163 kPa using Terzaghi's formula. Therefore, the bearing capacity factor of safety for the assumed ground with river embankment as shown in Fig. 14 is given by $F_s = q_{t,NC}/q = 16.7/13.6 = 1.23$. Substitution of this value for $S_{i,NC} (= 8.9$ cm), $F_s (= 1.23)$ and parameters, C , Λ and Λ_0 into Eq. (4b) yields the earthquake-induced immediate residual settlements of the embankment, depending on the magnitude of cyclic-induced excess pore pressures, u/p'_c . The variation of residual settlements, $\Delta S_{i,cy}$, calculated using Eq. (3) with u/p'_c is illustrated in Fig. 19, which indicates that the resid-

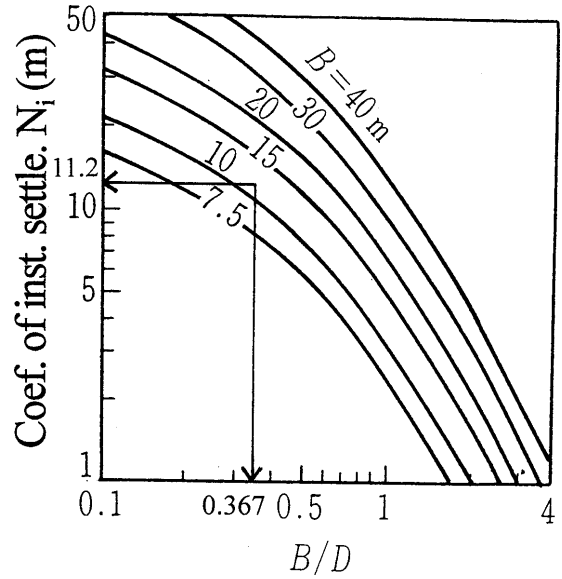


Fig. 16. Coefficient of instantaneous settlement plotted against B/D (after Inada et al., 1977)

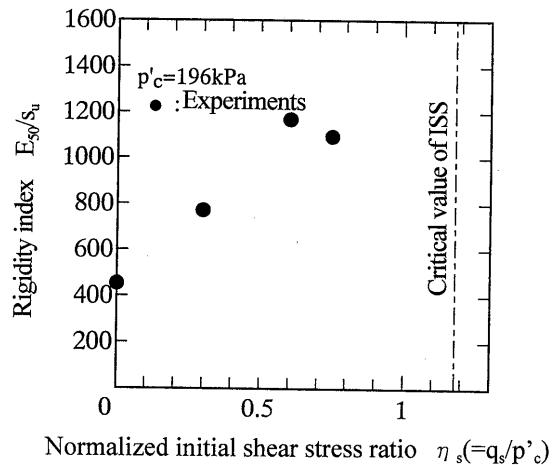


Fig. 17. Variation of rigidity index with initial shear stress ratio observed in undrained triaxial tests

ual settlement increases with increasing cyclic-induced excess pore pressure. In particular, it abruptly increases when u/p'_c approaches 0.5, and exceeds 1.0 m at a value of 0.6.

To determine precisely the distribution of earthquake-induced excess pore pressures in the ground beneath an embankment, a dynamic response analysis with a nonlinear stress-strain relation for the soil, such as YUSAYUSA proposed by Ishihara and Towhata (1980), should be performed using the actual acceleration records from strong earthquake motions. However, in the present study the cyclic-induced excess pore pressure is assumed to be uniformly distributed with depth, because this paper aims at demonstrating an example of the procedure of calculation using the proposed method. According to recent results from measurements at Port Island and a numerical analysis of the Great Hanshin

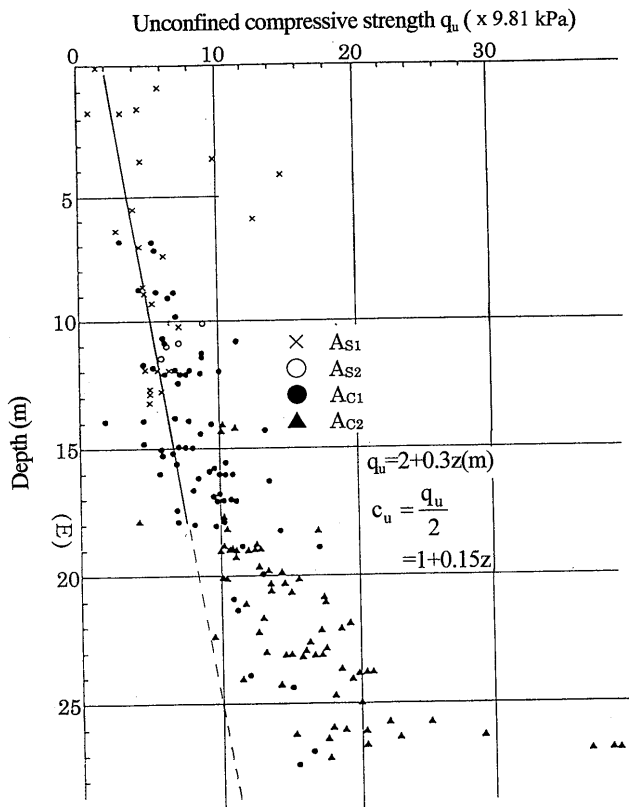


Fig. 18. Distribution of unconfined strength against depth at ground under the river dyke (after Matsuo et al., 1997)

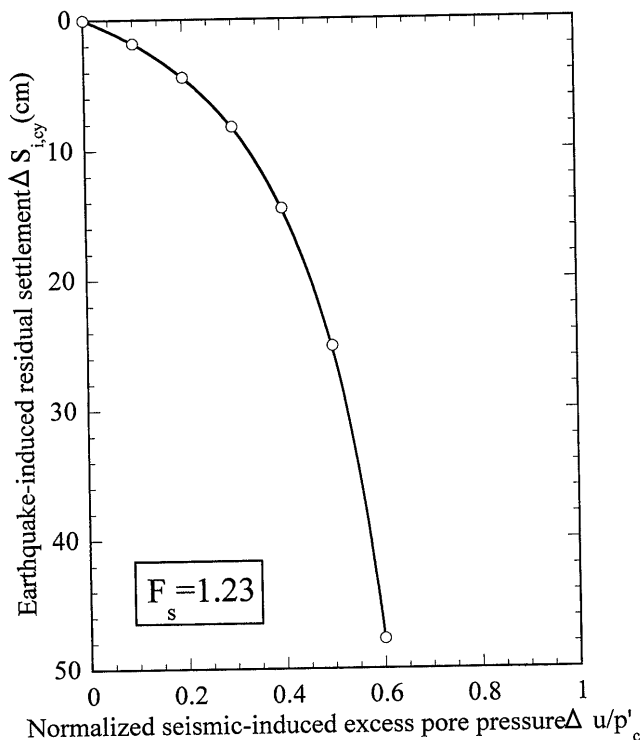


Fig. 19. Calculated earthquake-induced instantaneous settlements of embankment on silty clay

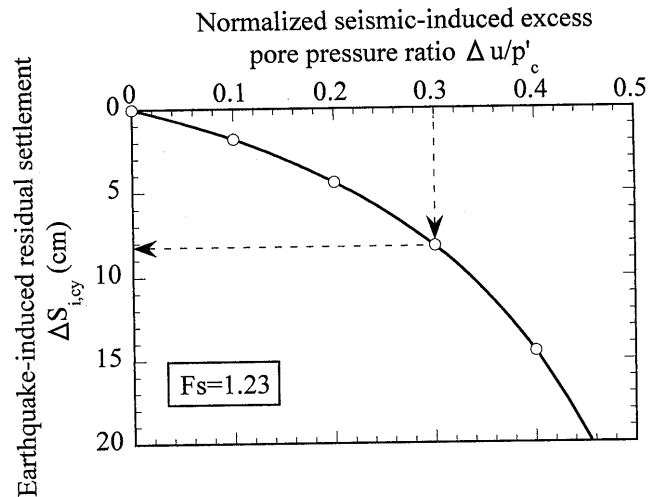


Fig. 20. Allowable and calculated earthquake-induced instantaneous settlements of embankment on silty clay

Earthquake in 1995 which was carried out by Fukutake (1996), earthquake-induced excess pore pressure normalized by the confining pressure was approximately 0.2 to 0.3. Referring to these results, let us here assume that the excess pore pressure ratio u/p'_c generated for the model ground during earthquakes is 0.3. Then, we obtain immediate residual settlement equal to 0.082 m from Fig. 20. It should be noted, however, that this result is based on the assumption (one-dimensional distribution of $u/p'_c = 0.3$ throughout the clay deposit underneath embankment) simplified for facilitating the calculation using the method proposed in the present paper. Hence, in order to estimate precisely, the two- or three distribution of u/p'_c which might occur during the actual earthquake should be determined using the reliable two- or three-dimensional dynamic numerical analysis. However, although this has been already done by the one of the author's group in a separate piece of research (Yokokawa, 1998), the results will appear in a separate paper in the future.

Let us here consider the effect of the bearing capacity factor of safety on the earthquake-induced immediate settlement of the model ground. Figure 21 demonstrates the influence of safety factor on the normalized earthquake-induced pore pressure versus residual settlement relations. Figure 21 shows that not only does the bearing capacity increase, but also the settlement is reduced with an increasing safety factor. In particular, if F_s is assumed to be 3.0, as is conventionally used for long-term bearing capacity, residual settlement falls within the allowable value, 0.15 m, for river banks as defined by the Ministry of Construction in Japan.

Settlement due to Dissipation of Earthquake-Induced Excess Pore Pressures

When the cyclic-induced excess pore pressure ratio, u/p'_c is 0.3, as mentioned in the previous section, the settlement due to dissipation of earthquake-induced excess pore pressures is: $\Delta S_{vt} = 30 \times \{0.225 \times 0.310 / (1 + 0.928)\}$

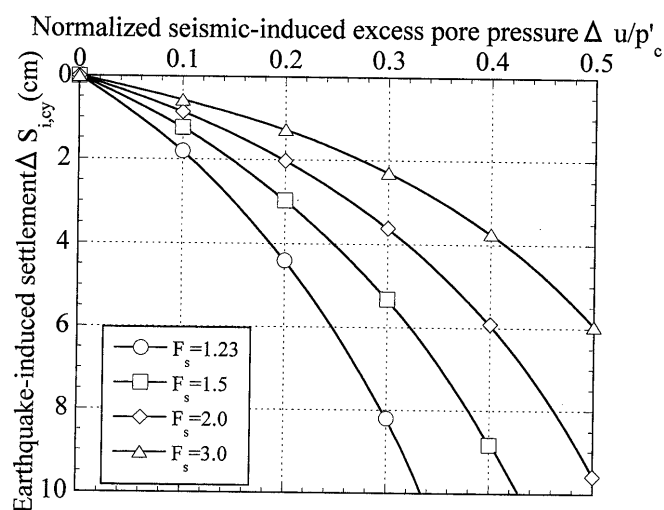


Fig. 21. Effect of safety factor on relation of $\Delta S_{i,ey}$ and $\Delta u/p'_c$

$\times \{\log 1/(1-0.3)\} = 0.168$ m. Thus, cyclic-induced total settlement is $\Delta S_{cy} = 0.082$ m + 0.168 m = 0.250 m (= 25.0 cm).

CONCLUSION

Based on methods previously presented by the authors (Yasuhara et al., 1992, 1994, 1996, 1997, 1998) for predicting the degradation in strength and stiffness of fine-grained soils in the course of undrained cyclic loading due to earthquakes, a methodology has been developed to estimate the cyclic-induced immediate settlements as well as post-cyclic recompression settlements due to the dissipation of cyclic-induced excess pore pressures in fine-grained soils. In addition to this, a simple example calculating the seismic-induced settlement of a river embankment founded on soft cohesive soils using the proposed procedure is described. It should be noted, however, that earthquake-induced immediate settlements included in the case history may have been overestimated because E_{50} was adopted for Young's modulus in the calculations. If we had used the real value for E determined from considerations of the non-linearity of stiffness, then we would have obtained a more realistic prediction of earthquake-induced settlement. A simplified method is proposed in the present paper where:

- 1) The earthquake-induced settlements depend on the cyclic softening of stiffness more than the reduction in strength.
- 2) The empirical formula for predicting the settlements is very simple, being based on a hyperbolic settlement versus load relation.
- 3) The method proposed here for predicting cyclic-induced settlement is given in terms of cyclic-induced excess pore pressures, plasticity index and bearing capacity factor of safety.

For the proposed method to be more useful for field engineers, it should contain a dynamic response analysis. In addition it is also necessary to consider the fact that the

strength and stiffness of sedimentary deposits of soft fine-grained soils generally vary with depth.

REFERENCES

- 1) Boulanger, R. W., Meyers, M., Mejia, L. H. and Idriss, I. M. (1998): Behaviour of a fine-grained soil during the Loma Prieta earthquake, *Can. Geotech. J.*, **35**, 146-158.
- 2) Fukutake, T. (1995): Three-dimensional liquefaction analysis of interaction among ground, foundation and structures, *Investigation Report of 1995 Hyogoken-Nambu Earthquake*, Technical Research Institute, Shimizu Construction Co. Ltd. (in Japanese).
- 3) Hyde, A. F. L. and Ward, S. J. (1985): A pore pressure and stability model for a silty clay under repeated loading, *Géotechnique*, London, England, **35** (2), 113-125.
- 4) Hyodo, M. et al. (1994): Undrained cyclic shear behaviour of normally consolidated clay subjected to initial static shear stress, *Soils and Foundations*, **34** (4), 1-12.
- 5) Iizuka, A. and Ohta, H. (1987): A determination procedure of input parameters for elasto-viscoplastic finite element analysis, *Soils and Foundations* **27** (3), 71-87.
- 6) Inada, M., Akaishi, M. and Chou, K. (1977): Shearing deformation of soft ground due to embankment, *Tsuchi-to-Kiso (J. JSSMFE)*, **25** (3), 53-56 (in Japanese).
- 7) Ishihara, K. and Towhata, I. (1980): One-dimensional soil response analysis during earthquakes based on effective stress method, *J. of the Faculty of Engrg.*, The University of Tokyo (B), 655-700.
- 8) Kusakabe, O. and Kawai, N. (1989): Reduction in bearing capacity and increase in settlement of a footing due to an upward seepage flow, *J. of JSSMFE (Tsuchi to Kiso)*, **37** (6) (377), 57-62 (in Japanese).
- 9) Lefebvre, G., Leboeuf, D. and Hornych, P. (1991): Slope failures associated with the 1988 Saguenay earthquake, Quebec, Canada, *Can. Geotech. J.*, **29**, 117-130.
- 10) Matsuda, H. (1998): Estimation of post-earthquake settlement-time relations of clay layers, *J. of Geotech. Engrg.*, JSCE, (568), III-39, 41-45 (in Japanese).
- 11) Matsui, T., Ohara, H. and Itou, T. (1980): Cyclic stress-strain history of and shear characteristics of clay, *J. Geotech. Engrg. Div.*, ASCE, **106** (19), 1101-1120.
- 12) Matsui, T., Bahr, M. A. and Abe, N. (1992): Estimation of shear characteristics degradation and stress-strain relation of saturated clay after cyclic loading, *Soils and Foundations*, **32** (2), 161-172.
- 13) Matsuo, O., Shimadzu, T. and Tamoto, S.: (1997): Study on seismic stability of levees on soft ground, *Doboku-gijyutu-shiryuu (Technical Report of Civil Engrg.)*, PWRI, **39** (9), 56-61 (in Japanese).
- 14) Mitachi, T. and Kitago, S. (1976): Change in undrained shear strength characteristics of saturated remoulded clay due to swelling, *Soils and Foundations*, J. of Japanese Geotech. Society, **16** (1), 45-68.
- 15) Noto, S. and Kumagai, M. (1986): An experimental study on dynamic properties of peat soils, *Monthly Report of Civil Engrg. Research Institute*, Hokkaido Develop. Bureau, (393), 12-21 (in Japanese).
- 16) Ohara, S. and Matsuda, H. (1990): Study on the settlement of saturated clay layer induced by cyclic loads, *Soils and Foundations*, **28** (3), 103-113.
- 17) Pradhan, Tej B. S., Dam L. D. K. and Shiokawa, M. (1997): Settlement analysis of clay deposit induced by earthquake motion, *Proc. 11th World Conf. Earthquake Engrg.*, **1**, (361).
- 18) Stark, T. and Contreas, I. A. (1998): Fourth Avenue landslide during 1964 Alaskan earthquake, *J. Geotech. and Geoenvironmental Engrg.*, ASCE, **124** (2), 99-109.
- 19) Suzuki, T. (1984): Settlement of soft cohesive ground due to earthquake, *Proc. 38th Annual Meeting on JSCE*, **III**, 87-88 (in Japanese).
- 20) Wroth, C. P. and Houslyby, G. T. (1985): Soil mechanics-Property

- characterization and analysis procedures, *Proc. 11th ICSMFE*, **1**, 1-56.
- 21) Yamaguchi, H. (1977): Panel Discussion, *Proc. 9th ICSMFE*, **3**, 382-384.
 - 22) Yasuhara, K., Hyodo, M., Konami, T. and Hirao, K. (1991): Earthquake-induced settlement in soft ground, *Proc. 2nd Intn'l Conf. Recent Advances in Geotechnical Earthquake Engrg. and Soil Dynamics*, **1** (3.9), 365-370.
 - 23) Yasuhara, K. and Andersen, K. H. (1991): Clay behaviour under consecutive long-term cyclic loading in direct simple shear tests, *Proc. ASCE*, (439/III-17), 9-16 (in Japanese).
 - 24) Yasuhara, K., Hirao, K. and Hyde, A. F. L. (1992): Effects of cyclic loading on undrained strength and compressibility of clay, *Soils and Foundations*, **32** (1), 100-116.
 - 25) Yasuhara, K., Oikawa, H. and Noto, S. (1993): Large strain cyclic behaviour of peat, *Proc. Intn'l Workshop on Advances in Understanding and Modelling the Mechanical Behaviour of Peat*, The Netherlands, 301-310.
 - 26) Yasuhara, K., Satoh, K. and Hyde, A. F. L. (1994): Post-cyclic undrained stiffness for clays, *Proc. Intn'l Symp. Prefailure Deformation of Geomaterials*, **1**, 483-489.
 - 27) Yasuhara, K. (1994): Post-cyclic undrained strength for cohesive soils, *J. Geotech. Engrg.*, ASCE, **120** (11), 1961-1979.
 - 28) Yasuhara, K. (1995): Earthquake-induced settlements in peaty ground, *Proc. Intern'l Workshop on Engrg. Characteristics and Behavior of Peat*, Sapporo, Japan, 5.1-5.9.
 - 29) Yasuhara, K. and Hyde, A. F. L. (1997): Method for estimating post-cyclic undrained secant modulus of clays, *J. Geotech. and Geoenvironmental Engrg.*, ASCE, **123** (3), 204-211.
 - 30) Yasuhara, K., Hyde, A. F. L., Toyota, N. and Murakami, S. (1997): Cyclic stiffness of plastic silt with an initial drained shear stress, *Géotechnique, Special Issue, Pre-Failure Deformation Behaviour of Geomaterials*, 371-382.
 - 31) Yasuhara, K. (1999): Discussion to "Behaviour of a fine-grained soil during the Loma Prieta Earthquake" by Boulanger, R. W., Meyers, M. W., Mejia, L. H. and Idriss, I. M. (CGJ, 36: 146-158, 1998), *Can. Geotech. J.*, **36**, 582-583.
 - 32) Yasuhara, K. and Murakami, S.: Dynamic FE analysis for stability of embankment on silty clay during earthquakes, (Unpublished).
 - 33) Yokokawa, S. (1997): Evaluation of residual deformation and instability of soft cohesive soils under earthquake loading, *MS Thesis*, Graduate School, Faculty of Engrg., Ibaraki Univ., (in Japanese).
 - 34) Zeevaert, L. (1987): *Foundation Engineering for Difficult Subsoil Conditions (2nd Edition)*, Van Nostrand Co., Ltd.